REPORT DOCUMENTATION PAGE

Form Approved
OMB NO. 0704-0188

1. AGENCY USE ONLY (Leave Blank)	2. REPORT DATE	3. REPORT TYPE AND DATES COVERED
		Final 01 May 01 - 30 June 04

4. TITLE AND SUBTITLE
Development of Acoustic Based, Multi-tasking Sensing and Actuation Capabilities for Gas Turbines

5. FUNDING NUMBERS
DAAD19-01-1-0571

6. AUTHOR(S)
Tim Lieuwen

7. PERFORMING ORGANIZATION NAME(S) AND ADDRESS(ES)
Georgia Tech
School of Aerospace Engineering
270 Ferst Drive, Atlanta, GA 30318

8. PERFORMING ORGANIZATION REPORT NUMBER
E-16-T70

9. SPONSORING / MONITORING AGENCY NAME(S) AND ADDRESS(ES)
U. S. Army Research Office
P.O. Box 12211
Research Triangle Park, NC 27709-2211

10. SPONSORING / MONITORING AGENCY REPORT NUMBER
41297.2-EG

11. SUPPLEMENTARY NOTES
The views, opinions and/or findings contained in this report are those of the author(s) and should not be construed as an official Department of the Army position, policy or decision, unless so designated by other documentation.

12 a. DISTRIBUTION / AVAILABILITY STATEMENT
Approved for public release; distribution unlimited.

12 b. DISTRIBUTION CODE

13. ABSTRACT (Maximum 200 words)

This program is developing acoustic techniques for non-intrusive sensing and actuation of gas flows. Controlling and/or monitoring the degree of mixing between constituents of a multi-component media is a key problem in a variety of applications. Monitoring such mixing processes necessarily requires capabilities for quantification of the level of "mixedness". However, quantification of *molecular* mixedness levels, as opposed to macro-scale entrainment, is difficult. Under this program, we have demonstrated the use of acoustic absorption measurements to characterize an average level of molecular mixedness between gases across the wave propagation path. This report presents the results of example calculations and experiments demonstrating the feasibility of this technique and the significant sensitivity of acoustic absorption levels upon gas mixedness ; e.g., measurements reported here show acoustic amplitude differences of up to a factor of ten between identical gas mixtures whose only difference is the level of mixedness of their constituent gases.

14. SUBJECT TERMS
Acoustics, Sensing, Gas Turbines

15. NUMBER OF PAGES
18

16. PRICE CODE

17. SECURITY CLASSIFICATION OR REPORT	18. SECURITY CLASSIFICATION ON THIS PAGE	19. SECURITY CLASSIFICATION OF ABSTRACT	20. LIMITATION OF ABSTRACT
UNCLASSIFIED	UNCLASSIFIED	UNCLASSIFIED	UL

Papers Submitted/Published :

Cottet, A., Lieuwen, T., Acoustic Absorption Measurements for Characterization of Gas Mixing, *AIAA Paper # 2003-3259* presented at the 9th AIAA Aeroacoustics Conference, May 2003.

Cottet, A., Lieuwen, T., Gas Mixing Diagnostics Using Acoustic Absorption Measurements, presented at 2003 Meeting of the Acoustic Society of America, Austin, TX, November, 2003

Cottet, A., Neumeier, Y., Scarborough, D., Bibik, O., Lieuwen T., Acoustic Absorption Measurements for Characterization of Gas Mixing, to appear in the Journal of the Acoustical Society of America, March 2004.

Scientific Personnel supported : Aurelien Cottet, GRA, Andrew Meyer, Research Engineer, Tim Lieuwen, Asst. Prof.

Report of Invention : Humidity/Water Vapor Concentration Sensor Using Acoustic Absorption Measurements, Invention Disclosure and provisional patent filed, GTRC ID 2876.

1 SUMMARY AND PROGRAM GOALS

The objectives of this program are to develop acoustic absorption techniques for gas flow diagnostics. The objective of this work was two fold: 1) determine the accuracy and sensitivity with which acoustic absorption can be measured in practical environments, and 2) demonstrate the use of acoustic absorption measurements to infer the level of molecular mixedness between constituents in a multi-component gas media. Controlling and/or monitoring the degree of mixing between constituents of a multi-component media is a key problem in a variety of applications. Monitoring such mixing processes necessarily requires capabilities for quantification of the level of "mixedness". However, quantification of *molecular* mixedness levels, as opposed to macro-scale entrainment, is difficult. This report demonstrates the use of acoustic absorption measurements to characterize an average level of molecular mixedness between gases across the wave propagation path. This approach takes advantage of the fact that over a large frequency range, acoustic damping is dominated by vibrational relaxation processes. The vibrational relaxation frequency for a particular gas is often a strong function of the other species it is in molecular contact with. Thus, the relaxation frequency of each species in a dual component gas mixture varies with the level of molecular mixedness of the constituent species. This report presents the results of example calculations and experiments demonstrating the feasibility of this technique and the significant sensitivity of acoustic absorption levels upon gas mixedness ; e.g., measurements reported here show acoustic amplitude differences of up to a factor of ten between identical gas mixtures whose only difference is the level of mixedness of their constituent gases.

2. INTRODUCTION

Controlling, enhancing and/or monitoring the degree of mixing between constituents of a multi-component media is a key problem in a variety of applications; e.g., in various chemical processes or in developing fuel/air mixers for low NOx combustors[1,2]. In particular, for applications where the rate of chemical reactions is controlled by the molecular collision rate between mixture constituents, control and/or enhancement of mixedness at the molecular level, as opposed to simply macro-scale entrainment, is needed. Optimization of such mixing enhancement strategies necessarily requires capabilities for quantification of the level of "mixedness". However, quantification of *molecular* levels of mixedness, as opposed to macro-scale entrainment, is difficult. For example, consider mixing assessment based upon visual assessment. Figure 1 shows a simulated gray-scale image of a two-species mixture at a low (left image) and high (right image) resolution levels. Completely dark and light regions correspond to pure levels of one specie or the other. Intermediate gray-scales correspond to various levels of mixing between the two. The point of the picture is to illustrate that the true configuration of the mixture constituents is difficult to asses from a visual or imaging system whose resolution is much less than that of the scale of a mean free path of molecular motion. A visual assessment of the system necessarily "mixes out" the true mixture features at a level below the system's resolution.

The objective of this work is to demonstrate an acoustic technique to characterize the level of gas mixedness at the molecular level. The use of acoustic absorption measurements as gas phase mixture diagnostics has received limited attention to date. The majority of existing acoustic diagnostic techniques have relied on sound speed or Doppler shift measurements to infer quantities such as average temperature, gas composition of binary mixtures, or gas velocity[3, 4, 5, 6]. Absorption measurements for diagnostic purposes have been reported in some recent studies for gas composition characterization[6] or particle sizing[7]. The technique described here is unique in that it based upon the fact that the relaxation frequency for a particular gas is often a strong function of the other species it is in molecular contact with. Thus, the relaxation frequency of a dual component gas mixture varies with the level of molecular mixedness of the constituent species.

Before proceeding to the detailed discussion, we provide a brief review of acoustic absorption via molecular relaxation processes. Acoustic absorption processes arise from viscosity, thermal conductivity, gas diffusion in multi-component mixtures, and rotational and vibrational relaxation of internal energy modes[8]. Of most interest here are vibrational relaxation processes, which damp acoustic waves through the following mechanism: the gas compression associated with the acoustic wave cause perturbations in the gas temperature and, thus, local translational energy. Through molecular collisions, the translational energy is redistributed to the rotational and vibrational degrees of freedom. During very low frequency acoustic perturbations, energy is fed from the translational to the vibrational energy modes of the gas during the compressive phase of the acoustic cycle. This energy is then returned from the vibrational to the translational energy modes during the rarefaction phase of the cycle. While gas translational and rotational modes equilibrate very quickly (generally within a few collisions), the vibrational mode requires extensively longer (several thousand collisions). Thus, even at relatively low frequencies the internal energy exchange processes cannot respond sufficiently quickly to acoustic fluctuations, with the affect that energy is not removed from or returned to the dilatational disturbance in phase with its oscillations. These nonequilibrium affects cause the acoustic wave to be damped. Maximum acoustic damping per wavelength of acoustic propagation distance occurs at the "relaxation frequency", f_v. An additional, relatively minor, affect of these nonequilibrium phenomenon is to slightly increase the speed of sound. Following Pierce[9], Figure 2 plots the dependence of the acoustic absorption and sound speed upon normalized frequency, f/f_v.

In the figure, the quantity α_v refers to the acoustic damping coefficient due to vibrational relaxation; i.e., a wave propagating through a distance x is reduced in amplitude by the factor $\exp(-\alpha_v x)$. Figure 2 shows that acoustic wave damping/per wavelength of propagation due to vibrational relaxation is maximum at the relaxation frequency, f_v, and reduced at higher and lower frequencies. The figure also shows that the speed of sound increases from its "equilibrium value" for $f << f_v$ to its "frozen value" when $f >> f_v$. In general this change in sound speed is quite small; i.e., a typical change is on the order of 0.1% of the nominal sound speed. The damping of acoustic waves by these vibrational relaxation processes is quite significant, however. *In fact, it is generally the dominant damping mechanism in gaseous media over a wide range of frequencies;* e.g., for frequencies less than about 1 MHz in air.

The fundamental principle motivating this study is the fact that the *relaxation frequency of a particular gas is often a function of the other species with which it is in molecular contact*. Numerous studies have demonstrated this point in various gases, such as nitrogen[10,11],

oxygen[12,13], carbon monoxide[14], and carbon dioxide[15]. For example, Figure 3 plots the dependence of the vibrational relaxation frequency, f_v, of carbon dioxide (CO_2) upon the concentration of ambient water vapor (H_2O), methanol (CH_3OH), and several other gases; e.g., it shows that f_v in CO_2 with 0 and 0.1% H_2O increases from 20 to 150 kHz.

As such, the relaxation frequency of a binary gas mixture can vary with the level of molecular mixedness of the constituent species. In other words, if the two gases are completely unmixed, the vibrational relaxation rates of each species are simply equal to their values in isolation. In contrast, if the gases are mixed, the relaxation frequency may have a different value that depends upon the relative constituent concentrations. The objective of this work is to demonstrate this point. The rest of the paper is organized in the following manner: The following section provides some example calculations using simulated mixedness profiles and tabulated relaxation frequency data. The objective of this section is to theoretically demonstrate the feasibility of the concept. Then, we present experimental results for CO_2-propane (C_3H_8) and CO_2- H_20 mixtures that verify the strong effect of mixedness levels upon acoustic absorption levels. Data included here shows that in some cases, the acoustic amplitude changes by a factor of ten between two identical gas mixtures, whose only difference is the level of mixedness of their constituent gases.

3 EXAMPLE CALCULATIONS

The objective of this section is to present example calculations illustrating the effects of gas mixedness on acoustic absorption using simulated mixedness profiles and standard acoustic absorption formulas. As in our experiments, CO_2 was chosen as the primary gas in this study. CO_2 was chosen because of its relatively low vibrational temperature (~950 K), resulting in high levels of absorption at room temperatures in the 10-90 kHz range (this frequency range was of interest because of the acoustic transducer available to us). Many other candidate species with higher vibrational temperatures (e.g., N_2 or O_2) have low levels of vibrational mode excitation at room temperature, making the total amount of absorption relatively small at these frequencies and over distances on the order of our experiment size, 18 cm.

For these simulations, we use water vapor as the second gas, because of the well characterized nature of its molecular interactions with CO_2. As shown in Figure 3, water vapor has a strong impact on the vibrational relaxation rate of CO_2.

These calculations use the following formula's presented by Pierce[9] for acoustic absorption and neglect the effect of absorption by gas diffusion. The total absorption coefficient, α, can be written as $\alpha = \alpha_{cl} + \sum_v \alpha_v$, where α_{cl} is the classical absorption coefficient. It represents the sum of the viscous and thermal absorption coefficients and is given by:

$$\alpha_{cl} = \frac{\pi\omega\eta}{c^2}\left(\frac{4}{3} + \frac{\eta_B}{\eta} + \frac{(\gamma-1)}{\mathrm{Pr}}\right) \tag{1}$$

where η, η_B, γ, Pr, c, and ω denote the viscosity, bulk viscosity, ratio of specific heats, Prandtl number, sound speed, and angular frequency, respectively. We used values of c= 266 m/s, η = 0.000085 m^2/s, Pr = 0.78 and $\frac{\eta_B}{\eta} = 0.6$ in these calculations[9]. Note that the above equations assume that the frequency is much less than the rotational and translational relaxation

frequencies, a reasonable assumption for the frequencies of interest here. The vibrational absorption coefficient , α_v , was computed from:

$$\alpha_v = \left[\frac{\pi(\gamma-1)}{\gamma}\frac{1}{\lambda}\right]\left[\frac{C_{v,V}}{C_V}\right]\left[\frac{\omega\tau_v}{1+(\omega\tau_v)^2}\right], \quad (2)$$

where τ_v and $\frac{C_{v,V}}{C_V}$ denote the vibrational relaxation time and specific heat due to the vibrational modes, normalized by the total specific heat. Note that the fundamental principle behind the technique described here is the dependence of this relaxation time, τ_v, upon mixedness level. Baseline plots of the dependence of the absorption coefficient upon frequency and water vapor concentration are shown in Figure 4. The figure shows that, at a fixed H_20 level, the absorption coefficient monotonically increases with frequency. Note, however, the non-monotonic dependence of the absorption coefficient upon H_20 level at a fixed frequency. This non-monotonicity is due to the shift in relaxation frequency with H_20 level.

For an actual absorption measurement, the total amount of absorption must be neither negligible nor too large because of signal/noise considerations; e.g., it is difficult to distinguish between disturbances with levels that are 99.9% and 99% of their original values in the former and 0.1% and 0.01% in the latter cases. As such, the optimal frequency range for absorption measurements depends upon the spatial distance between the source and receiver. Figure 5 plots the total absorption, $\exp(-\alpha y)$, across a distance y=18 cm, corresponding to the size of the experiment described in the next section. The nonlinear dependence of the acoustic absorption level upon (in this case) H_20 content shown in the figure is key to the technique being pursued here. Because of this nonlinearity, the total absorption of a sound wave traversing the medium depends upon the local concentration values, and not just the integrated sum across the line of sight. If these relations were purely linear, the absorption level would not change with mixedness levels. For example, consider the mixing of equal parts of a pure CO_2 and CO_2+ 0.1% H_2O mixture, such that the final mixture consists of CO2 + 0.05% H_20. Figure 5 shows that the difference in absorption levels between the mixed and unmixed states is relatively small at frequencies below about 30 KHz, but rapidly increases at higher frequencies.

To quantify the change in absorption levels with mixing, consider a spatially inhomogeneous mixture of CO_2 and H_2O, where the spatial profile of the H_2O is plotted in Figure 6. Figure 7 plots the dependence of the acoustic absorption upon mixedness levels at several frequencies. The mixedness value indicated in the figure was quantified by linearly scaling the ratio of the profile's standard deviation to its mean, σ/μ , between zero and unity. At each frequency, the absorption level is normalized by its value in the perfectly mixed case. We use the integrated absorption $\exp\left(-\int \alpha dy\right)$ to determine the total absorption (i.e., we assume negligible acoustic reflections). The figure shows that rather large differences exist (factors up to ~20) between the wave amplitude in the perfectly mixed and unmixed cases. These differences become much smaller, however, at mixedness levels above about 75%. This example clearly shows the plausibility of absorption measurements to characterize gas mixedness levels.

4. EXPERIMENTAL FACILITY

Having theoretically demonstrated the feasibility of gas mixedness characterization using acoustic absorption measurements, we next describe companion experiments to demonstrate the

technique. A photograph and drawing of the facility are shown in Figure 8. It consists of an 244 cm long, 20 x 28 cm section aluminum duct that is capped at one side and open at the other side. A translating box 30.5 x 27.9 x 6.4 cm with one open end slides inside the duct. All joints in the duct are sealed with an RTV silicone to prevent contamination of the mixture inside. Although removed for the photograph, a nozzle is fitted to the end of the box to minimize back diffusion of gas from the ambient air into the box. This nozzle is fitted to flexible hosing connected to the building exhaust. Two gases of arbitrary composition, denoted as Gas "A" and Gas "B", flow through the main chamber and the translating box and mix at the translating box exit. Great effort was expended to maintain a "clean" flow so that the two gases mix in a steady, laminar fashion. In order to minimize flow unsteadiness and flow separation, the translating box was fabricated to have an aerodynamic profile. First, its width tapers down at the back to a thin edge so that the outer flow can cleanly divide around it. In addition, the edge of the box where the two gases initially mix is machined to a 0.05 cm width to minimize the wake thickness.

For this experiment, gases "A" and "B" simply consisted of two CO_2 sources with different levels of some secondary gas. We used both H_20 and propane (C_3H_8) as the secondary gases. Water vapor was used because of the abundance of existing data on its effect on CO2 vibrational relaxation rates. However, as will be discussed further below, the substantially different molecular weight between it and CO_2 introduced a host of measurement problems. For this reason, the majority of data was taken with C_3H_8, which has essentially the same molecular weight as CO_2. Dry, industrial grade CO_2 (99.98% purity, < 10 ppm water vapor) flows through the main part of the chamber and around the translating box (Gas A). In cases where H_20 was used as the secondary gas, CO_2 was humidified by passing it through a bubbler. Its humidity was systematically varied by mixing the relative concentrations of this stream with a second dry CO_2 stream, which is then introduced through the translating box. H_20/CO_2 mass ratios of 0-0.3% were achieved with this arrangement. The water vapor concentration was measured with a Tri-Sense relative humidity sensor, model EW-37000-00. In cases where C_3H_8 was used as the secondary gas, a flow control panel was used to mix the desired concentrations from 0 to 20% by mass of C_3H_8 in CO_2. The C_3H_8 concentration was measured via a custom infrared absorption technique that was set up for this experiment. Gas was removed from the measurement volume via a 1.3 cm diameter sampling probe. Light from a broadband (2.5-14 μm) thermal radiation source was passed through the gas in a cell and into an infrared spectrometer set at 3.3 μm, the approximately wavelength of maximum C_3H_8 infrared absorption (CO_2 absorption at this wavelength is negligible). The dependence of the spectrometer output voltage to C_3H_8 concentration was determined from off-line calibration experiments that spanned the C_3H_8 ranges encountered in these experiments.

All gas flows are metered with calibrated rotameters with velocities from 1 - 5cm/s. These velocities were determined from diffusive mixing calculations, with the requirement that the two gases could be completely mixed when the translating box is positioned the farthest distance from the transducer (120 cm). As such, the degree of gas mixing can be varied via the box location and/or the gas velocity.

Acoustic disturbances are generated with a 38mm diameter, type 616341 electrostatic Polaroid transducer. Acoustic measurements are obtained with a 1/8" type 4191 Bruel and Kjaer microphone. The speaker and microphone are situated near the downstream end of the duct and can be seen in Figure 8. The gas was acoustically interrogated by either driving the transducer with a persistent sinusoidal signal or with bursts of 10-50 acoustic cycles at the desired frequency, followed by a pause in order to allow the reverberant field to damp out, as illustrated

in Figure 9. The latter technique was used in early experiments (where water vapor was used as the secondary gas) but side-by-side comparisons with the persistent excitation technique showed the acoustic amplitudes at the microphone were essentially identical. As such the measurements with C_3H_8 as the secondary gas used a persistent excitation.

5. PROPANE CALIBRATION MEASUREMENTS

Our literature review did not find data on C_3H_8 effects on CO_2 relaxation rates, so we obtained extensive calibration data of these mixtures, in order to be able to compare our unmixedness measurements to a theoretical value. This procedure was not needed for CO_2-H_2O mixtures, because of the extensive data that already exists; e.g., see Figure 3. We obtained these calibration data by measuring the acoustic absorption between 30-90 kHz across uniform flowing mixtures in the facility shown in Figure 8, using propane levels ranging between 0-20% by mass. These data are shown in Figure 10. In order to facilitate theoretical predictions, we fitted these data by assuming the absorption is only due to CO_2. While this fit is most physically meaningful at lower C_3H_8 concentrations, it nonetheless provides a convenient method for collapsing the absorption data into a simple set of coefficients for insertion into a theoretical model. Rather than attempting to back out an absorption coefficient by determining the amplitude at two different wave propagation distances with the appropriate diffraction corrections, we normalized the measured amplitude at each C_3H_8 concentration level by the amplitude using pure CO_2. The best fit value of the relaxation frequencies at each propane level were determined using these data and Eqs. (2-3). The resulting curves are plotted with the data in Figure 10, as well as the calculated relaxation frequencies that were used to generate them in Figure 11. Figure 10 shows that the theoretical line satisfactorily fits the data, except in the 70-90 kHz regions at the two highest C_3H_8 levels, probably for the reasons given above. Note also that the fitted relaxation frequency in the 0% C_3H_8 case does not equal its pure value of 20 kHz, as shown in Figure 3, but rather 47 kHz. Using the results shown in Figure 3, this suggests that the "pure" CO_2 in these experiments actually contains about 100 ppm water vapor.

6. UNMIXEDNESS RESULTS

In a typical experiment, two initially unmixed gas streams enter the facility in the positions noted in Figure 8. At the point where gas A exits the translating box, it mixes with gas B. As these gases convect down the duct and mix, the acoustic amplitude is measured at different axial locations, accomplished by pulling the translating box away from the transducers.
Typical transverse C_3H_8 concentration profiles at different axial locations are shown in Figure 12. The two vertical lines indicate the edges of the translating box. It can be seen that the profile at the translating box exit is smoothed out somewhat from the discontinuous change in concentration, at least partially due to the averaging of the 1.3 cm diameter measurement probe in the transverse direction. As expected, the profiles smooth out with increasing axial mixing distance, and at 120 cm, the propane concentration is completely uniform. Ideally, the total integrated C_3H_8 concentration across the flow at each axial location should stay nearly constant. Typical differences were on the order of 1-5%, but never more than 10%, providing some indication of the accuracy of these measurements.

The typical dependence of the acoustic amplitude upon axial mixing distance, normalized by its values at the perfectly mixed x = 120 cm axial location, are shown in Figure 13. The figure shows the substantial, generally monotonic, increase in acoustic amplitudes as the gases become more mixed. Data are not shown for 80 or 90 kHz because the absorption was so high that the

amplitude could not be accurately measured in all cases. The dependence of the ratio of the acoustic amplitude in the most unmixed and mixed, A(x=0)/A(x=1.2 m), cases upon frequency is plotted in Figure 14 (the result from another test with a slightly higher propane concentration is also included). It shows that the acoustic amplitude increases by a factor of roughly 2 and 10 in the 30 and 70 kHz cases, making the point that the effect of mixedness upon acoustic amplitude is by no means minor! The figure also shows a comparison of the predicted dependence of this ratio upon frequency, calculated using the measured absorption at each C_3H_8 level in the perfectly mixed case and assuming that the total absorption could be approximated as $\exp\left(-\int \alpha dy\right)$. The two results have similar qualitative trends, although the theoretical predicted frequency sensitivity of the amplitude ratio is significantly less than what was experimentally observed. These differences are due in part to the sensitivity of the theoretical result to the exact details of the C_3H_8 profile. For example, the true profile likely changes much more sharply at the translating box edges, but is smeared out somewhat in the measurements because of the transverse averaging of the measurement probe. We ran sensitivity studies to evaluate the manner in which the predicted amplitude ratio would change with deviations in C_3H_8 profile. By using a "flat-top" exit profile whose concentration changed discontinuously from 2% in the outer flow to 8.25% in the translating box, the frequency sensitivity changed to approximately 0.85 and 0.35 at 30 and 70 kHz, respectively. These values are much closer to our measurements. Analogous data were obtained for the case where water vapor was used at the secondary gas. In these studies, we were not able to make accurate measurements of the transverse water profile concentrations due to the poor sensitivity of our humidity sensor at the low concentrations used. In addition, humidity levels and pressure amplitude measurements were often very unsteady. Obtaining good, repeatable data from this facility was challenging because of the strong role of buoyancy effects at these low flow velocities. Consequently, we were only able to obtain reasonable data under rather limited conditions where the H_20 concentration remained relatively steady. Note that the H_20 concentration tends toward a vertically stratified profile (i.e., highest water concentrations at the top) at large mixing distances.

Figure 15 illustrates the dependence of the 30 - 60 kHz acoustic amplitude, normalized by its value at x=1.0 m. It shows a monotonic decrease in acoustic amplitude with increased mixedness. The amplitude of the errorbar corresponds to the fluctuation level of the signal. Note that the decrease in amplitude observed here, compared to the increase observed in the above data, is simply due to the concentration levels of the secondary gas; opposite trends can be observed with either gas at other concentration levels. The dependence of the ratio of the acoustic amplitude at the two axial extremes (A(x=0)/A(x=1.0 m) cases upon frequency is plotted in Figure 16. As above, the errorbar indicates the level of fluctuation of the signal amplitude. It shows that the acoustic amplitude decreases by a factor of roughly 1.5 and 4 in the 30 and 60 kHz cases.

7. CONCLUDING REMARKS

This work has theoretically and experimentally demonstrated the feasibility of using acoustic absorption measurements to characterize levels of gas mixedness along a line of sight. While the theoretical validation data shown here deliberately focused on steady state, laminar mixing cases so that the corresponding gas concentration profiles could be readily measured, we have obtained ample data in cases where unsteady mixing is clearly prominent. For example, by intentionally causing the flow velocities of the outer flow and the translating box to differ we

could observe what is apparently the unsteady rollup of the shear layer between the two streams. This behavior can be seen in Figure 17, where the average velocity of the outer flow has intentionally been set 60% higher than in the translating box. Pure CO_2 is used in both flows in curve (1) to illustrate that the amplitude is essentially constant in the absence of unsteady species mixing, illustrating that the bouncing observed in the signal amplitude in other cases is not due to velocity fluctuations. Approximately 30% propane is added to the translating box flow in curves (2-7), which are taken at successive axial locations downstream. At the translating box exit (curve 2), the signal oscillates only slightly. The level of oscillations (as well as the average amplitude) grows monotonically with downstream distances of 5, 15, and 30 cm. The unsteadiness in amplitude is particularly evident at 30 cm. The amplitude of oscillations then decreases with further distance, indicating that the two streams are nearly mixed. Although not shown, at 120 cm the signal is essentially flat with no bouncing.

In closing it should be pointed out the implementation of the technique is gas specific, depending upon the nature of the vibrational-translational and vibrational-vibrational interactions between the gases being mixed. The technique may not work in all situations, such as with two monotonic gases or two gases with little effect upon each other's vibrational relaxation rates. However, a possible way to extend the technique to such cases would be to mix one or more of the gases with a third gas that does impact the other's relaxation rates.

8. FIGURES

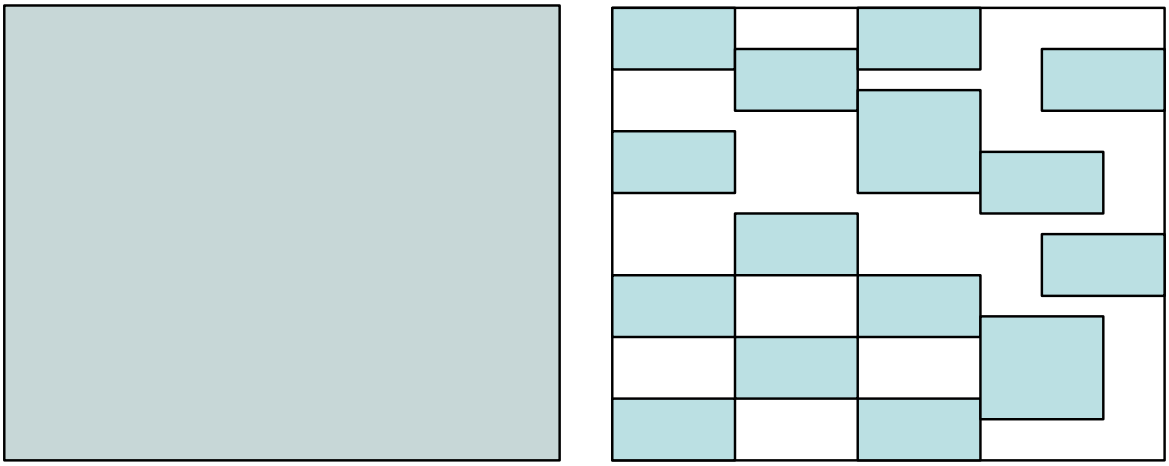

Figure 1. Simulated photograph of two-specie mixture at two resolution levels.

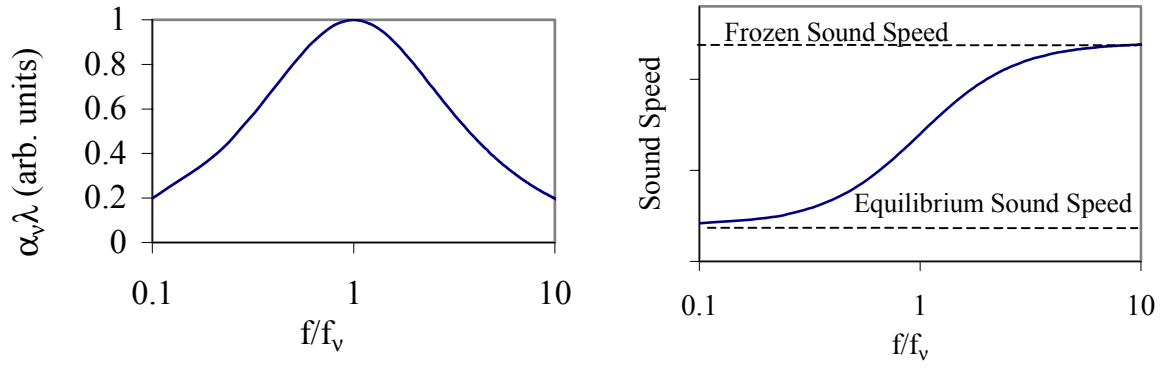

Figure 2. Dependence of the acoustic absorption and sound speed upon the normalized frequency.

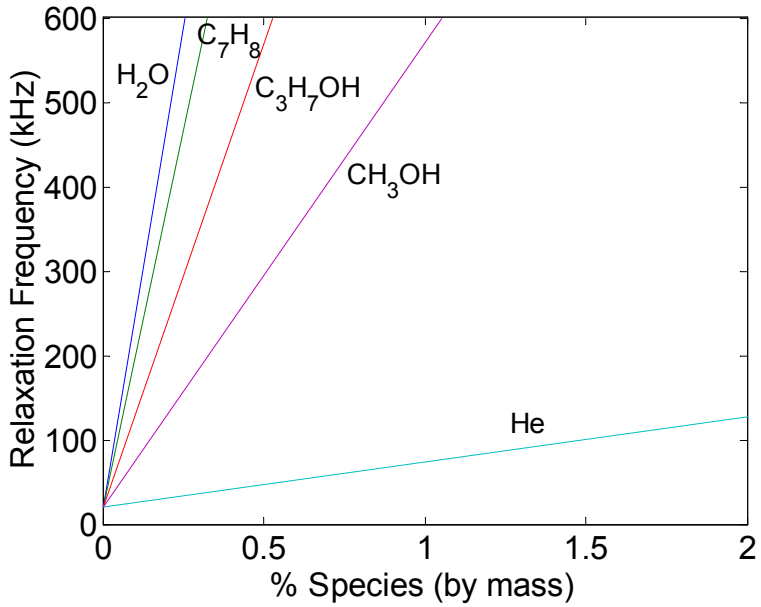

Figure 3. Dependence of f_v in carbon dioxide mixtures with the indicated species. Data obtained from Knudsen and Fricke[16].

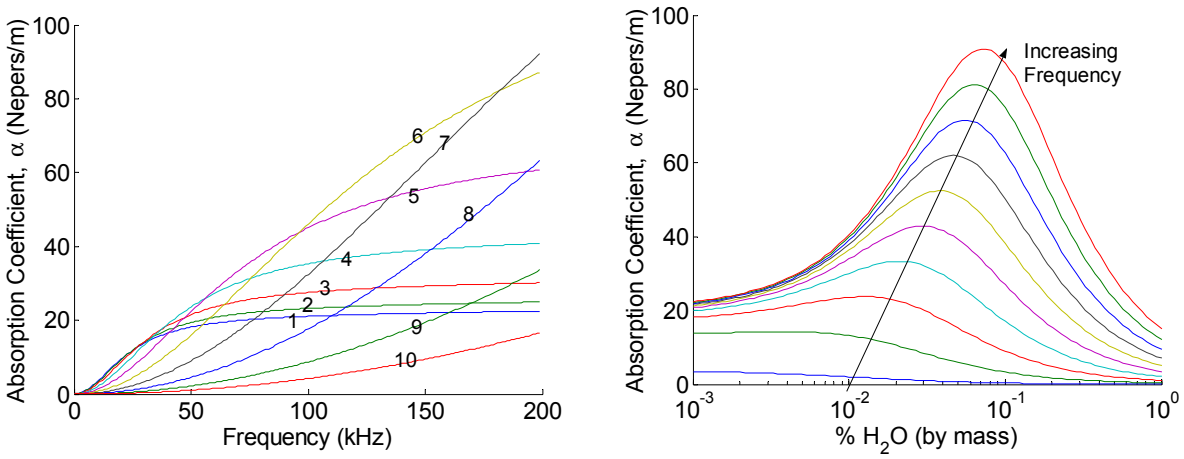

Figure 4. Dependence of total acoustic absorption coefficient upon frequency for several CO_2-H_2O mixtures; curves numbered to indicate (left) H_2O levels of 0.001, 0.002, 0.005, 0.01, 0.02, 0.05, 0.1, 0.2, 0.5, and 1% by mass and (right) frequencies of 10, 30, 50, 70, 90, 110, 130, 150, 170, and 190 kHz

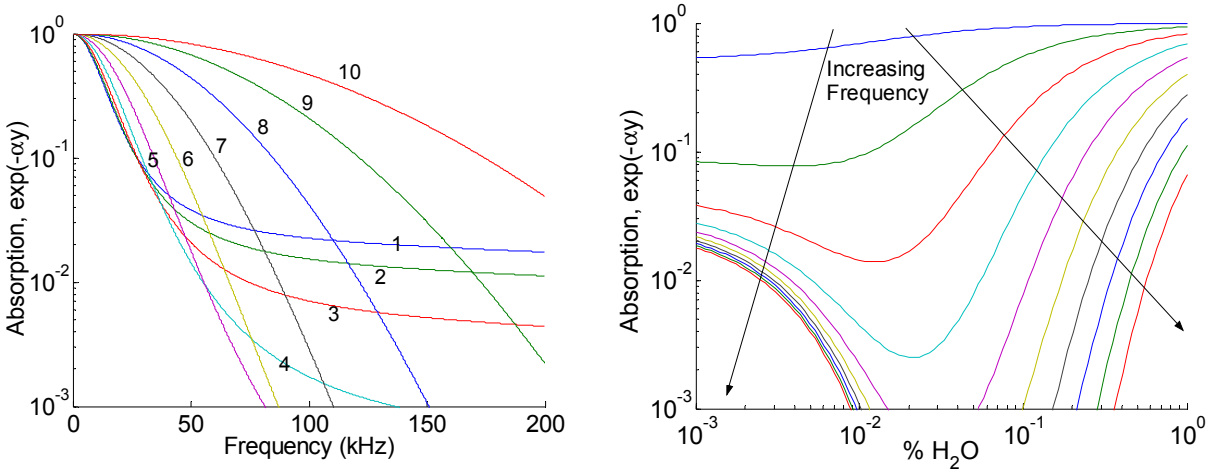

Figure 5. Dependence of total acoustic absorption, $\exp(-\alpha x)$, across a distance x=0.18 m upon frequency for several CO_2-H_2O mixtures; curve numbering same as in Figure 4.

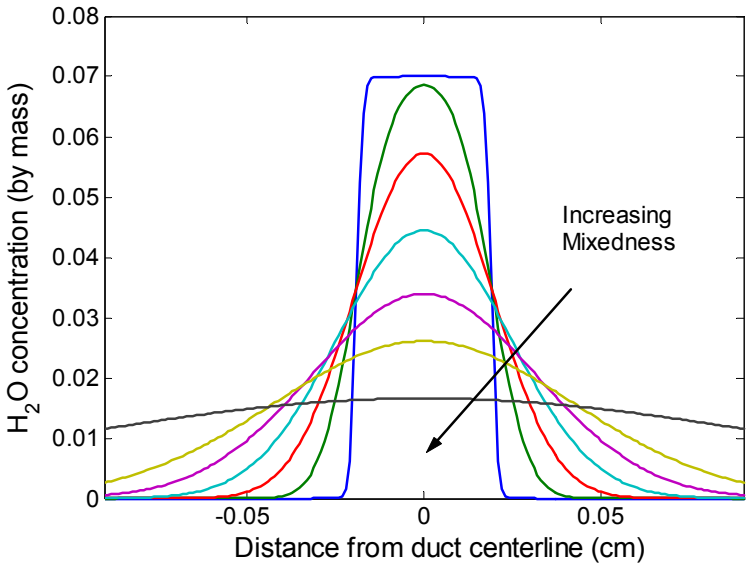

Figure 6. Assumed spatial dependence of H_2O mixedness level for model problem. Line points in the direction of increased mixedness.

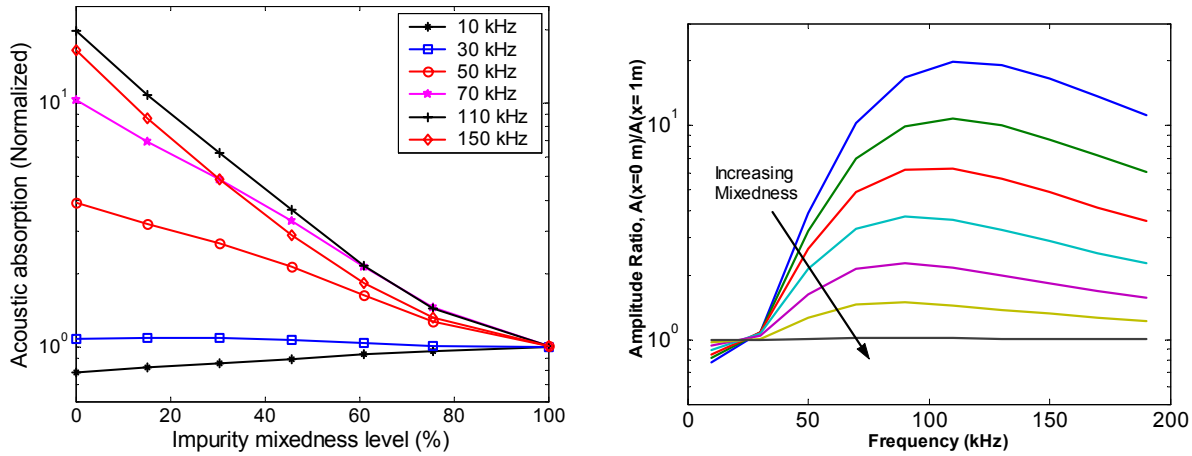

Figure 7. Dependence of acoustic absorption, (left) upon mixedness levels at frequencies of 10, 30, 50, 70, 90, 110, 130, and 150 kHz and (right) upon frequency at different mixedness levels; mixedness level same as in Figure 6

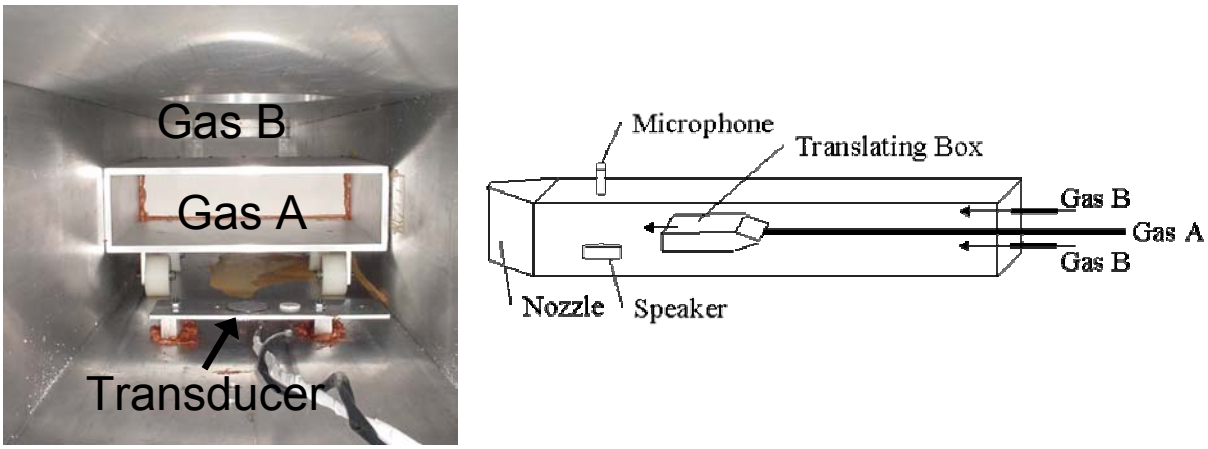

Figure 8. Photo (flow coming out of page) and drawing of facility developed for acoustic absorption measurements.

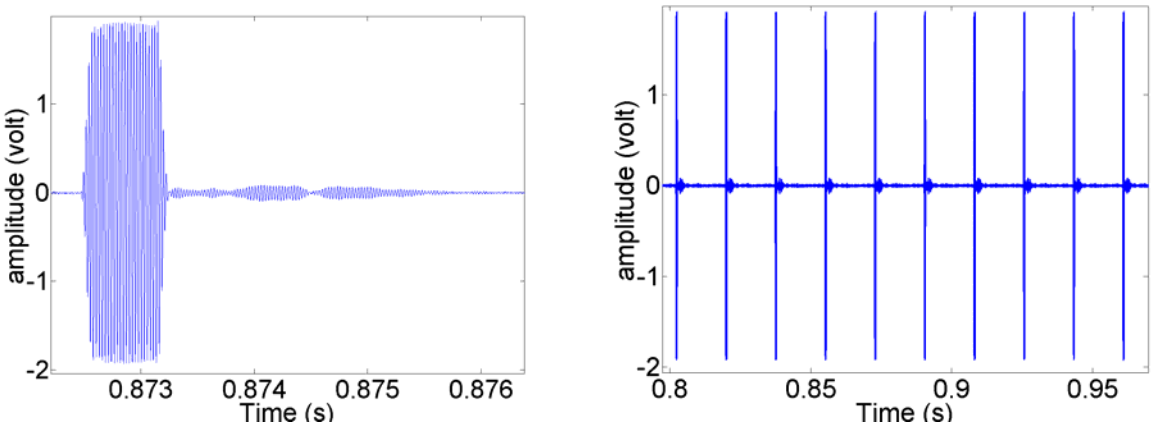

Figure 9. Time dependence of acoustic pressure, illustrating spaced tone bursts at two different time resolutions. Top image shows a detail of a single burst, illustrating subsequent echoes.

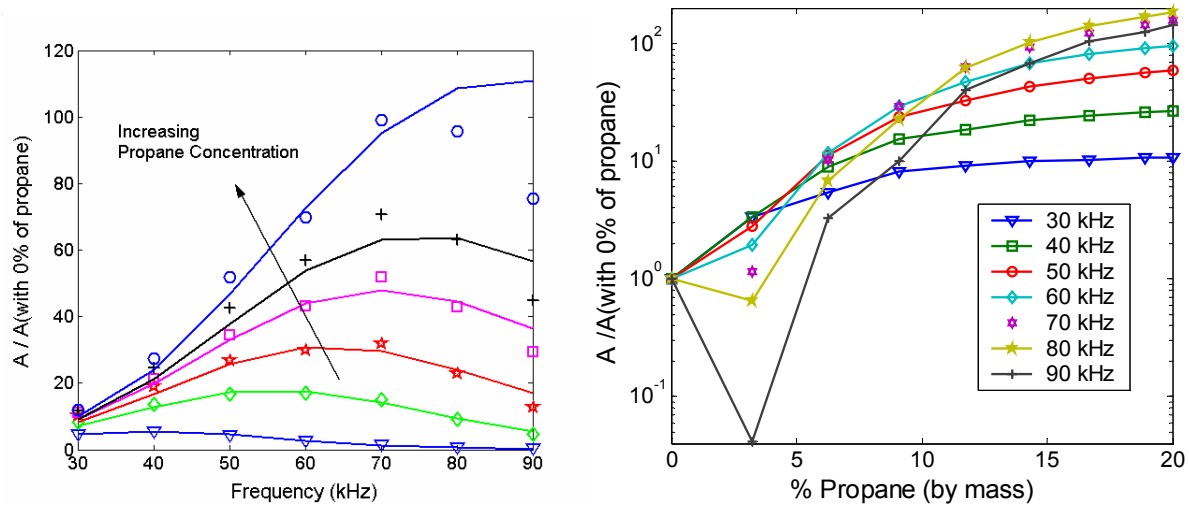

Figure 10. Dependence of measured (symbols) and, in left plot, fitted (line) acoustic amplitude at the indicated propane concentration, normalized by its pure CO_2 value at C_3H_8 concentrations of 0, 3.2, 6.3, 9.1, 11.7, 14.3, 16.6, 18.9, 20% (2 cm/s axial flow velocity). Only measured data is shown on right.

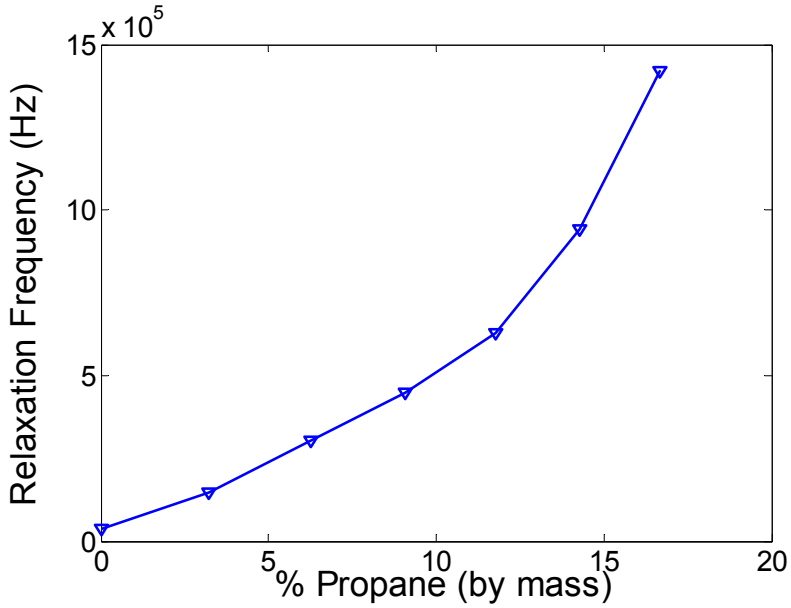

Figure 11. Measured dependence of f_ν in C_3H_8-CO_2 mixtures.

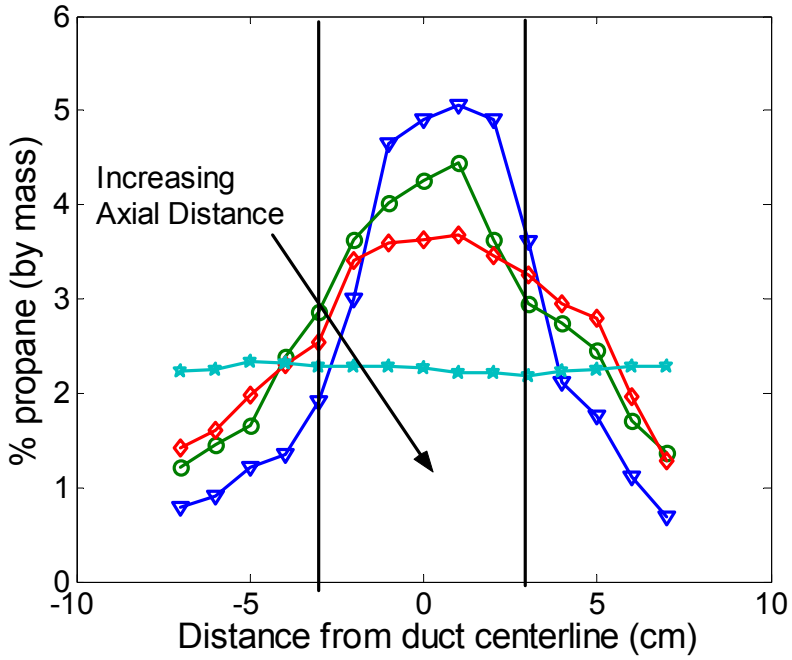

Figure 12. Measured transverse propane concentration profile at mixing distances of 0, 2.5, 5 and 120 cm (axial flow velocity = 3 cm/s). Vertical lines denote translating box edges.

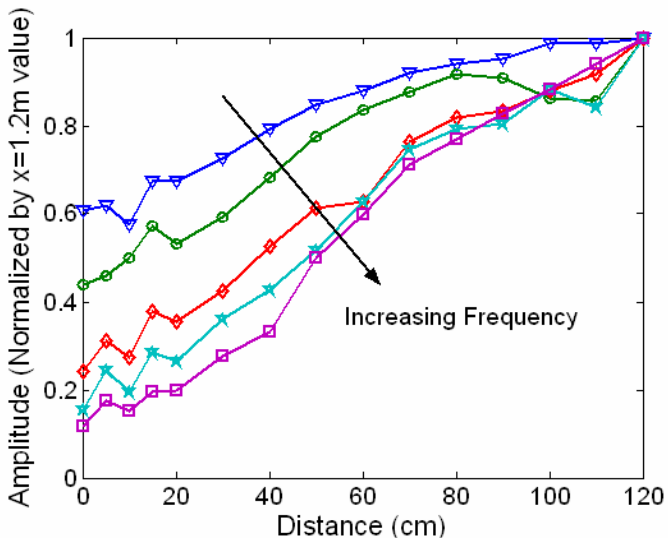

Figure 13. Dependence of 30, 40, 50, 60 and 70 kHz amplitude signal upon axial distance between gas stream origination point and acoustic transducer (initial propane concentration of 8.5%, axial flow velocity = 3 cm/s).

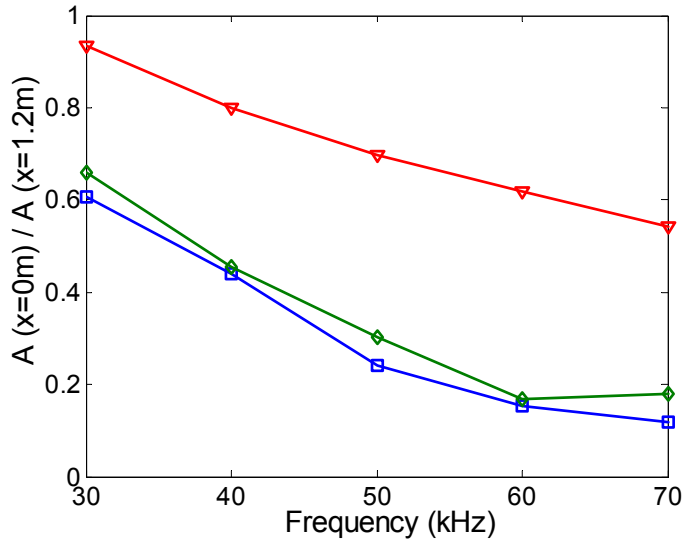

Figure 14. Comparison of theoretical, ∇, (based upon measured C_3H_8 concentration at box exit in 8.5% propane case) and measured (initial C_3H_8 concentrations at translating box exit of 8.5%, ◊, and 9.4 %,) ratio of acoustic amplitude at x=0 and 120 cm. Axial flow velocity = 3 cm/s

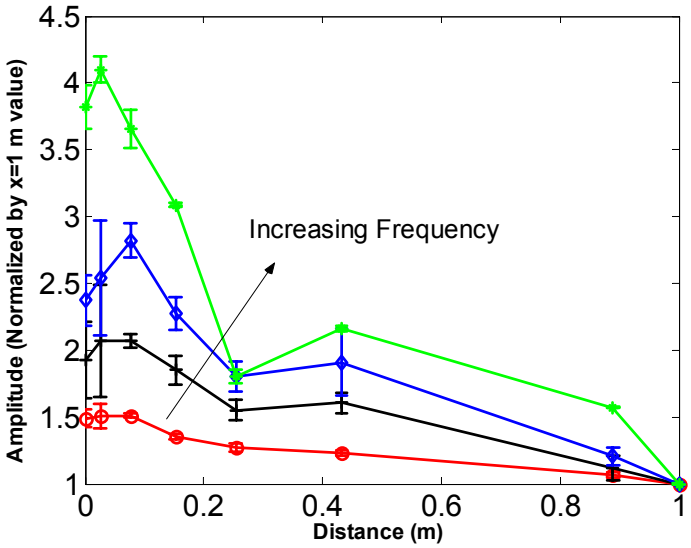

Figure 15. Dependence of 30, 40, 50, and 60 kHz amplitude signal upon axial distance between gas stream origination point and acoustic transducer (approximate water vapor concentration at translating box exit is 0.045%).

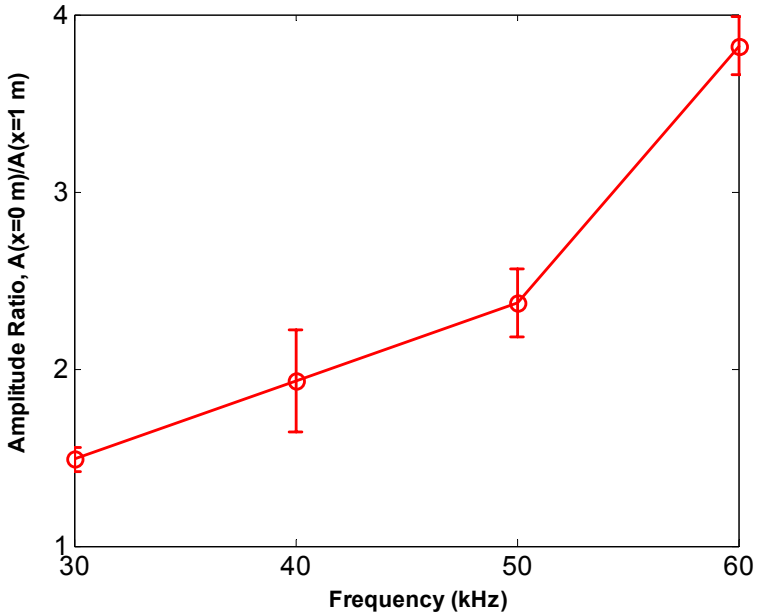

Figure 16. Dependence of ratio of acoustic amplitude at x =0 and 100 cm upon frequency. Errorbars denote level of fluctuation of signal.

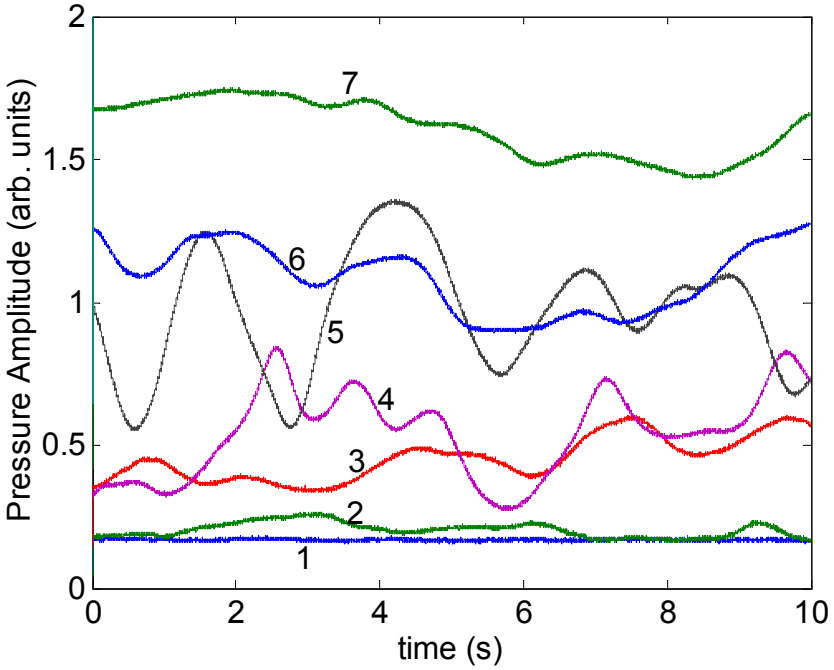

Figure 17. Temporal dependence of amplitude of 50 kHz signal with (1) pure CO_2, and (2-7) C_3H_8-CO_2 mixtures at axial distances of x=0, 5, 15, 30, 40 and 60 cm (average velocities of 1.3 and 2.1 cm/s in the translating box and outer flow, respectively; 30% propane in translating box flow in cases 2-7).

9 REFERENCES

[1] Oldshue, James, *Fluid Mixing Technology*, Chemical Engineering: New York, 1983.

[2] Lefebvre, A.H., *Gas Turbine Combustion*, Edwards Brothers: Ann Arbor, 1999.

[3] Wright, W, Schindel, D, Hutchins, D, Carpenter, P, Jansen, D, *Ultrasonic tomographic imaging of temperature and flow fields in gases using air-coupled capacitance transducers*, J. Acoust. Soc. Am., 104 (6), 1998, p. 3446.

[4] Mori, M, Takeda, Y, Taishi, T, Furuichi, N, Aritomi, M, Kikura, H, *Development of a novel flow metering system using ultrasonic velocity profile measurement*, Experiment in Fluids, 2002, pp. 153 - 160

[5] Winter, H., Mair, E., Schoenework, H., *Device for Monitoring the Concentration of an Air-Vapor Mixture*, U.S., Patent 4,424,703, 1984.

[6] Phillips, S, Dain, Y, Lueptow, R, *Theory for a gas composition sensor based on acoustic properties*, Meas. Sci. Technol. 14, 2003, pp. 70-75

[7] Mougin,P, Wilkinson,D, Roberts, K, Tweedie, R, *Characterization of particle size and its distribution during the crystallization of organic fine chemical products as measured in situ using ultrasonic attenuation spectroscopy*, J. Acoust. Soc. Am., 109 (1), 2004, p. 274.

[8] Bhatia, A., *Ultrasonic Absorption*, Dover Publications: New York, 1967.

[9] Pierce, A., *Acoustics: An Introduction to its Physical Principles and Applications*, Acoustical Society of America: New York, 1991.

[10] Millikan, R., White, D., *Vibrational Energy Exchange Between N_2 and CO. The Vibrational Relaxation of Nitrogen*, J. Chem. Phys., Vol. 39(7), 1963, pp. 1803-1808.

[11] Bauer, H., Roesler, H., *Relaxation of the Vibrational Degrees of Freedom in Binary Mixtures of Diatomic Gases*, in *Molecular Relaxation Processes*, Academic Press: New York, 1966.

[12] White., D., Millikan, R., *Vibrational Relaxation of Oxygen*, J. Chem. Phys., Vol. 39(1), 1961, pp. 98-101.

[13] White, D., Millikan, R., *Vibrational Relaxation in Air*, AIAA J., Vol. 2, 1965 pp, 1844-1846.

[14] Von Rosenberg, C., Taylor, R., Teare, J., *Vibrational Relaxation of CO in Nonequilibrium Nozzle Flow, and the Effect of Hydrogen Atoms on CO Relaxation*, J. Chem. Phys., Vol. 54(5), pp. 1974-1987.

[15] Cottrell, T., Day, M., The *Effect of Noble Gases on Vibrational Relaxation in Carbon Dioxide*, in Molecular Relaxation Processes, Academic Press: New York, 1966.

16 Knudsen, V., Fricke, E., J. Acoust. Soc. Am., Vol. 5, Vol. 12, 1940, p. 255